Acta Scientiarum

http://periodicos.uem.br/ojs
ISSN on-line: 1807-8664
Doi: 10.4025/actascitechnol.v45i1.58733

CIVIL ENGINEERING

Influence of mean value of the modulus of elasticity in compression parallel to the grain on the design of timber trusses

Arthur Filipe Freire Gomes[1*], Fernando Menezes de Almeida Filho[1], Júlio Cesar Molina[2], Fernando Júnior Resende Mascarenhas[3], Francisco Antônio Rocco Lahr[4] and André Luis Christoforo[1]

[1]Departamento de Engenharia Civil, Universidade Federal de São Carlos, Rodovia Washington Luiz, s/n., 13565-905, São Carlos, São Paulo, Brazil. [2]Departamento de Engenharia Industrial da Madeira, Universidade Estadual Paulista, Itapeva, São Paulo, Brazil. [3]Departamento de Engenharia Civil, Centro de Inovação e Competência Florestal, Universidade de Coimbra, Coimbra, Portugal. [4]Laboratório de Estruturas de Madeira, Departamento de Engenharia de Estruturas, Escola de Engenharia de São Carlos, Universidade de São Paulo, São Carlos, São Paulo, Brazil. *Author for correspondence. E-mail: arthurfreire2009@gmail.com

ABSTRACT. The Brazilian standard ABNT NBR 7190 (*Associação Brasileira de Normas Técnicas* [ABNT], 1997) recommends adopting the mean value of the modulus of elasticity to compression in the direction parallel to the grain ($E_{c0,m}$) in the calculation of displacements. The values of wood stiffness vary considerably, and they can generate displacements above the limit (L 200^{-1}, where L is the span) established by the referred standard, which contributes to the appearance of pathologies in the structure. To evaluate the influence of the adoption of $E_{c0,m}$ in the calculation of displacements, mechanical properties of wood species were obtained experimentally. With the aid of numerical models and experimental values, ten types of trusses were analyzed (Porch, Inclined Chord, Top Inclined Chord, Parallel Chord, Bowstring, Fink, Howe, K Truss, Pratt, Scissor), three spans (5, 10, and 20 m) and two species (*Hymenolobium petraum* Ducke e *Hymenolobium* sp). Initially, adopting $E_{c0,m}$ for all members and performing a linear analysis, the maximum loads for the displacement L 200^{-1} were determined. Subsequently, experimental stiffness values were randomly assigned to each bar, and the maximum displacements were determined through nonlinear geometric analyses. Based on 1260 numerical simulations, deflections of approximately 17% (span of 5 m), 30% (span of 10 m), and 34% (span of 20 m) were observed to be higher than the result considering $E_{c0,m}$. This problem can be overcome by using non-destructive methods in the pre-classification of the structure bars, positioning the elements rationally in the regions of the highest demand.

Keywords: dicotyledons; mechanical and physical properties; finite element method.

Received on April 19, 2021.
Accepted on May 17, 2022.

Introduction

It is difficult to imagine structures such as castles and cathedrals and several modern buildings with no timber elements. Notably, alongside stone and clay, wood has been used for thousands of years as a building material, and this use is motivated by its abundance and facility of handling it with simple and rustic tools (Almeida et al., 2016; Cavalheiro et al., 2016; Zangiácomo, Christoforo, & Lahr, 2016). In addition to being a renewable material, wood demands low energy consumption in its processing, and it has excellent potential for use in civil construction (Matos, Silva, Gama, Vale, & Rocha, 2012; Ter Steege et al., 2016; Tuisima-Coral, Odicio-Guevara, Weber, Lluncor-Mendonza, & Lojka, 2017). Furthermore, the leading cause of collapses in timber structures is human error (Dietsch, 2011), and not a failure due to the material itself, evidencing the quality of the wood as a material of construction.

Like the other structural materials, it is necessary to know wood species' physical and mechanical properties (Trevisan, Tieppo, Carvalho, & Lelis, 2007). To design safe, repairable, and efficient structures, designers must be able to characterize the properties of the materials accurately to be used in construction (Bukauskas et al., 2019). Therefore, for the design and analysis of timber structural elements, it is necessary to carry out tests to characterize their physical and mechanical properties.

Wood is a heterogeneous material, and its planting region and other factors can influence its physical and mechanical properties. Thus, structural parts may have their modulus of elasticity and strength significantly below the mean values. Therefore, the structure can present excessive displacements, uniquely if bars with mechanical and physical properties below the mean are placed in the most requested points of the structure.

Wood can be found as several structural elements, especially in roofs. In the last two decades, the diversity and sophistication of techniques used in constructing these structures have increased significantly (Bukauskas et al., 2019). The arches, beams, and trusses stand out among the possible structural roofing systems. Flexible connections are usually adopted using two or three pins in the trusses.

In timber roof trusses, exaggerated displacements stand out as one of the main pathologies (Andrade Junior et al., 2014). A possible cause of excessive displacements can be caused by the adoption of a $E_{c0,m}$ for all elements of the truss in the verification of the service limit states (maximum displacement of L (span) 200^{-1}).

In Brazil, the use of wood as a structural element is regulated by the technical standard NBR 7190 (ABNT, 1997), 'Design of Timber Structures', from the Brazilian Association of Technical Standards (ABNT). Among the guidance provided by this code, it is recommended to adopt the mean value of the compression modulus of elasticity in the direction parallel to the grain ($E_{c0,m}$) to analyze service limit states. According to this code, when evaluating the service limit state, the maximum displacement of timber structures is limited to the value L 200^{-1}, in which L is the distance between supports (span length).

According to Sandak, Sandak and Riggio (2015), wood deterioration occurs during their service life, which can be caused by mechanical, environmental or biological agents. Also, the deterioration of the wood can considerably affect its characteristics (Calil Júnior et al., 2006). Thus, it is essential to properly maintain and process the timber elements to avoid losing their properties. Some previous works present in the literature had the purpose of analyzing pathologies in timber structures.

Andrade Junior, Almeida, Stamato, Christoforo, and Lahr (2012) carried out inspections on a roof built with native Brazilian wood Piquiarana to analyze pathologies' appearance after a decade of use. In addition to this, the authors aimed to determine the strength and density properties of samples of the structure. Visual analyzes were carried out to assess the presence of pathologies and possible causes. Moreover, laboratory tests of samples were made to determine the mechanical properties of the wood. The main problems found were related to the design and execution of the work. No pathologies were found, and this was possibly due to the use of highly durable wood and the absence of direct contact with water.

Pinheiro, Lázaro, Macedo, Christoforo, and Lahr (2016) analyzed a timber roof truss through an inspection to identify pathologies and point out possible causes and solutions for them. The measures, type of used wood, the inspection of the conditions of the structure elements, such as the details of assembly, stability, and deformation of the elements, deterioration of the conditions of use of the structure, among others, were evaluated '*in loco*'. Pathologies such as deterioration of the structure, rupture, and instability of bars and connections, global instability, and excessive vertical displacement were found. Deterioration by biological agents, design, and execution errors were the leading causes, and preventive maintenance was recommended every 3 and 5 years.

Andrade Junior et al. (2014) evaluated the integrity of a warehouse's roof structure for chemical products. Inspections were carried out to assess possible pathologies in the elements of the structure and connections. Due to the lack of original designs, samples of the structure for determining the apparent density and some apparent properties were taken. The main problems were humidity, deterioration of the wood, poorly placed dowels, lack of braced frames, and deterioration of nails. The leading cause was the lack of maintenance of the structure.

Macchioni and Mannucci (2018) described the main characteristics of Italian trusses and their main pathologies. After investigating different structures, the problems were divided into three categories: failures in the connections, usually related to overload or decay of mechanical properties; bar failures, possibly due to the poor wood quality or sizing error; and decay of properties due to attacks by biotic agents. It was observed that the failures were usually accompanied by excessive displacement of the structure.

Excessive displacements can compromise the functioning of the structure itself or other parts of the building, so it is essential to understand these causes to increase the building's useful life. One of the reasons for excessive displacement may be the lack of projects, as reported by Andrade Junior et al. (2012) and Pinheiro et al. (2016). Among several recommendations of the Brazilian code, it highlights adopting the mean value of the modulus of elasticity to compression in the direction parallel to the grain for all the structure's bars. Due to the variability of the wood properties, this recommendation can cause vertical displacements higher than the limit (L 200^{-1}), which can cause pathologies. One method to control part of this problem is using non-destructive methods to estimate the members' stiffness. Among the various methods, it can be pointed out stress waves, ultrasound, transverse, and longitudinal vibration, and these methods have been the target of several kinds of research. Studies indicate the effectiveness of the methods mentioned above, with determination coefficients of up to 99% found for several non-destructive methods, such as tension waves

(Ballarin, Palma, & Hellmeister, 2010; Garcia et al., 2012; Chen & Guo, 2016; Yang, Jiang, Hse, & Liu, 2017), ultrasound (Haines, Leban, & Herbé, 1996; Mori, Hasegawa, Yoo, Kang, & Matsumura, 2016; Branco, Souza, & Tsakanika, 2017) and vibration: (Ballarin & Palma, 2009; Segundinho et al., 2013; Faydi, Brancheriau, Pot, & Collet, 2017; Guan, Liu, Zhang, Wang, & Zhou, 2019; Martins, Dias, & Cruz, 2019; Castellanos, 2020).

To evaluate the influence of adopting the mean value of the modulus of elasticity in compression parallel to the grain, a numerical study of 10 typologies was carried out (Porch, Inclined Chords, Top Inclined Chords, Parallel Chord, Bowstring, Fink, Howe, K Truss, Pratt, Scissor) and three spans (5, 10 and 20 m) and two wood species (Angelim Pedra - *Hymenolobium petraeum* Ducke and Angelim Ferro - *Hymenolobium* sp.). As recommended by the ABNT NBR 7190 (ABNT, 1997), the exact value of $E_{c0,m}$ was adopted for all bars in the reference model studied. Experimental values were randomly allocated in the structure bars in the other models. In total, 1260 numerical models were evaluated.

Material and methods

To determine the strength and stiffness of the wood, compression and tensile tests were performed on 100 specimens of each species according to the methodology for specimens free from defects presented in Annex B of the ABNT NBR 7190 (ABNT, 1997). All mechanical tests described below were performed with the aid of the Amsler machine with a capacity of 250 kN (Figure 1). The pieces of wood were stored in the Wood and Timber Structures Laboratory (LaMEM) in the Structures Department of São Carlos School of Engineering of the University of São Paulo, following all the procedures required by ABNT NBR 7190 (ABNT, 1997). The moisture content presented was close to 12%, and subsequently, the samples were chosen and tested in that same place.

To evaluate the displacements of the timber structures considered, some factors were defined. Ten types of trusses, three spans, and two wood species were evaluated. For each combination of factors, 21 variations were analyzed: 1 for reference, being carried out a linear analysis with $E_{c0,m}$ assigned for all bars; and 20 models, for which a nonlinear geometric analysis was performed, where the modulus of elasticity of each bar was randomly assigned. A summary of the factors is presented in Table 1, which were evaluated based on 1280 numerical models.

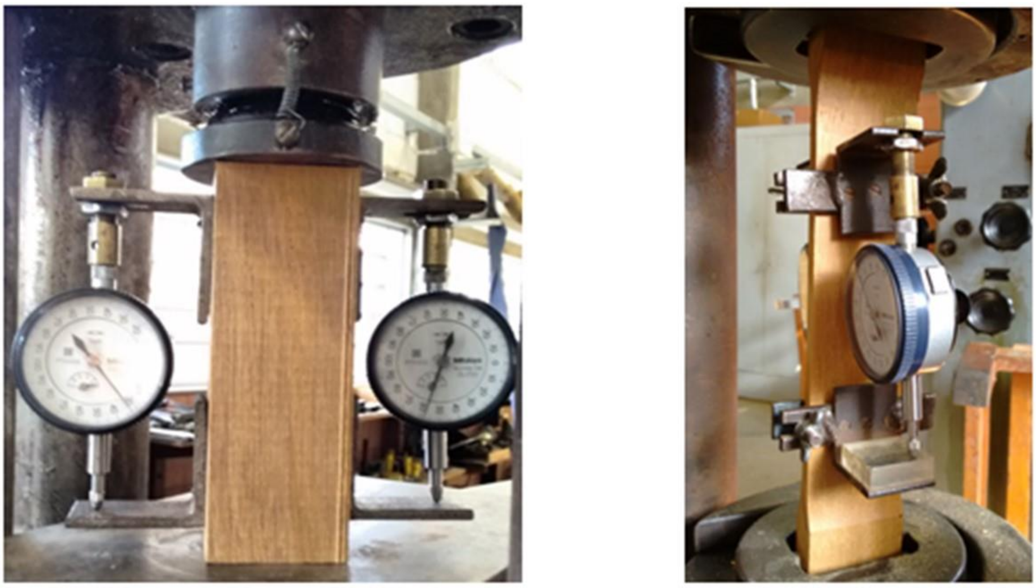

(a) (b)

Figure 1. Specimens positioned on the testing machine: (a) compression parallel to the grain and (b) tensile parallel to the grain.

Table 1. Analyzed factors.

Typologies	Pratt, Howe, Fink, Bowstring, Porch, Scissors, Top Inclined Chords, Inclined Chords, Parallel Horizontal Chords, K Trusses
Span (m)	5, 10 e 20
Species	Angelim pedra and Angelim ferro
Variations by model	Reference model: $E_{c0,m}$ (average value of the experimental values) + 20 models: $E_{experimental}$ randomly assigned to each bar

The trusses covered in the study were isostatic. Therefore, the stress in all the bars subjected to compression was verified based on the reference model ($E_{c0,m}$) to ensure that it was less than the elastic buckling load proposed by Euler (Equation 1), where E refers to the modulus of elasticity, I the moment of inertia and L the length of the bar. There are several normative aspects used to carry out checks on the stability and safety of the structure. In Brazil, the guidelines for the design of timber structures are provided by ABNT NBR 7190 (ABNT, 1997). However, as the research objective was to analyze the influence of the same stiffness for all members, it was not to carry out all the necessary checks for the design of the structures.

$$P_{cr} = \frac{\pi^2 EI}{(KL)^2} \quad (1)$$

To define the load and the cross-section for each model, the slenderness (λ), defined by Equation 2 of the compressed parts, was limited to 80. After modeling and processing the model, all measurements of the truss elements were obtained, and, based on maximum slenderness, the same cross-section was defined for all the bars of the structure, with square sections with multiple faces of 10 mm being chosen. In the next step, based on a linear analysis, the required load for the structure to reach the displacement limit in the service limit state stated as L 200^{-1}, was defined. After this stage, the compressed bars stress was compared to those proposed by Euler's formula (Equation 1). If any bar has higher values than the limit, the cross-section sides were increased by 10 mm, and a new load was defined. Once the reference model was defined, the same load was used in all subsequent analyzes.

$$\lambda = \frac{L}{r} \quad (2)$$

To compare the displacements obtained by the methodology proposed by ABNT NBR 7190 (ABNT, 1997) and a situation closer to reality, two species were characterized (Angelim Pedra and Angelim Ferro). The experimental values of stiffness and strength of each species were obtained (Table 2). Based on the experimental values, the E_{c0m} was calculated for each species, which was assigned to all the reference truss bars of each type, as recommended by the Brazilian standard.

To evaluate possible differences in the displacement values estimated by the methodology proposed by the standard and the real values, it was necessary to randomly assign the mechanical properties of the bars. Thus, the bars of each truss were numbered, and a cell was linked in Excel for each one. For this cell, a value from 1 to 50 was arbitrarily assigned using the 'RANDBETWEEN' function, available in Excel. Subsequently, each bar's mechanical properties were assigned using the 'IF' and 'PROCV' functions. The first function indicated whether the bar was subjected to compression or traction. The second function was used to return the bar's modulus of elasticity value. Part of a table used to define the stiffness of the bars is shown in Table 3. This attribution process reflects the conditions present in the construction sites, where the bars are assembled without any pre-classification.

Table 2. Mechanical properties of samples.

Sample	ρ_{ap} (kg m^{-3})	f_{c0} (MPa)	f_{t0} (MPa)	E_{c0} (MPa)	E_{t0} (MPa)
1	690	48	61	11178	10747
2	640	52	62	10155	9729
3	630	48	62	9932	9959
...	...	...	...	...	...

Table 3. Mechanical properties of bars.

Bar	Sample	E
1	43	11011
2	7	18226
3	37	20968
...	...	...

The Finite Element Method (FEM) stands out among numerical methods, discretizing the continuous domain and analyzing each subdomain individually. With the aid of the ABAQUS® software, analyses of the proposed models were carried out. The elements were created in a two-dimensional space using deformable wires. In the second stage, the mechanical properties of the wood (f_{co}, f_{t0}, E_{co}, E_{t0}) were defined and attributed to all the truss bars. In the third stage, the types of truss support and loading points were defined. All trusses were supported by two supports, one pinned and another roller. The loads were applied to the three central nodes of the top chord. The type of analysis to be performed was defined in the fourth step, with the general static type in all models. However, geometric nonlinearities were not considered in the reference models ($E_{co,m}$ adopted in all bars). The other nonlinear geometric models were considered using the 'Nlgeom' option, available in the ABAQUS® library. In step five, the elements were discretized by defining the mesh and the finite elements used. As in the studied trusses, the bars were considered pinned ends, and the loads were applied to the nodes. The stress obtained was constant throughout all the bars. As a result, each bar was discretized by a T2D2 element (two-node linear displacement element). A summary of the modeling steps is shown in Figure 2.

Loading was defined as 3-point loads applied to the top nodes of the truss and located in the center of the span (L/2), with the second and third points defined at L/4 distances to the left and right, respectively, from the center of the span. The maximum height of the models was defined as L/7. The numerical models, the loading application points, and the support positions are shown in Figure 3. The stopping criterion was defined as the convergence of the model adopting the minimum increment of 10^{-5}. From the values of the displacement obtained by the simulations, the Confidence Interval was elaborated (at the level of 95% reliability), seeking to establish the margin of uncertainty of the values of displacements obtained.

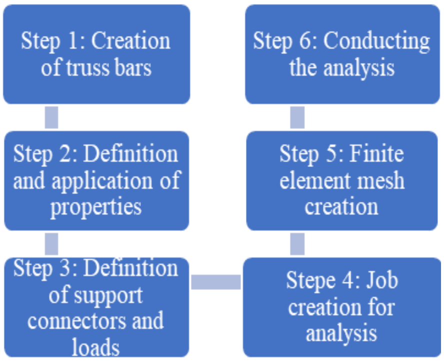

Figure 2. Flowchart of modeling in ABAQUS®.

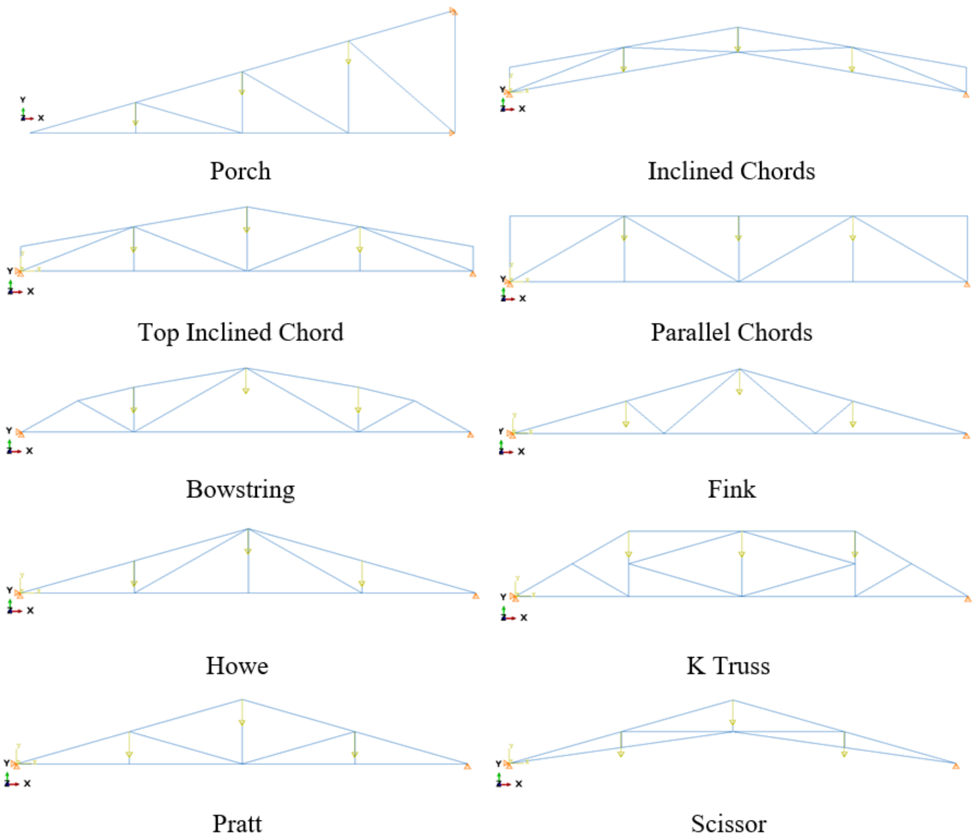

Figure 3. Typologies, loading points, and supports.

Results and discussion

Table 4 shows the mean values (X_m), the coefficients of variation (CV), and the lowest (Min.) and the highest (Max.) values of the properties investigated in the characterization of the two wood species considered in the present study. The values obtained experimentally were compared with values available in the literature, as shown in Table 5 and 6.

Based on the values found in the literature, it was possible to state that the data found in this study were consistent, showing slight variation from the available studies. Table 7 and 8 show the results of the analysis of variance (ANOVA - 5% significance) carried out to verify the equivalence of the modulus of elasticity obtained from the compression (E_{c0}) and tensile (E_{t0}) tests in the direction parallel to grain established by the Brazilian standard ABNT NBR 7190 (ABNT, 1997) for the woods of Angelim Pedra and Angelim Ferro, respectively. Figure 4 and 5 show the ANOVA validation tests (normality and homogeneity of the residual variance), with DOF - degrees of freedom; SQ - sum of squares; QM: mean of squares; F value - F statistic; P-value - P statistic.

Table 4. Property results for the two wood species considered.

Proprieties	Angelim Pedra				
	ρ_{ap} (kg m^{-3})	f_{c0} (MPa)	f_{t0} (MPa)	E_{c0} (MPa)	E_{t0} (MPa)
X_m	660	54.78	73.64	11,516	11,709
CV (%)	6.87	15.83	25.80	18.41	22.28
Min.	590	38.12	34.61	11,603	9,975
Max.	800	81.25	109.07	14,831	13,258
f_{wk} (MPa)	------	39.40	47.18	------	------
Proprieties	**Angelim Ferro**				
	ρ_{ap} (kg m^{-3})	f_{c0} (MPa)	f_{t0} (MPa)	E_{c0} (MPa)	E_{t0} (MPa)
X_m	1160	79.24	110.58	20,648	19,586
CV (%)	4.09	12.83	23.09	16.16	19.72
Min.	1040	53.00	87.00	18,135	16,011
Max.	1290	97.00	147.00	23,238	22,354
f_{wk} (MPa)	------	58.72	74.26	------	------

ρ_{ap} - apparent density at 12% moisture content; f_{c0} - compressive strength in the direction parallel to the grain; f_{t0} - tensile strength in the direction parallel to the grain; E_{c0} - compression modulus of elasticity in the direction parallel to the grain; E_{t0} - tensile modulus of elasticity in the direction parallel to the grain.

Table 5. Results of properties obtained by different authors - Angelim Pedra.

Authors	$\rho_{ap\ (12\%)}$ (kg m^{-3})	f_{c0} (MPa)	f_{t0} (MPa)	E_{c0} (MPa)	E_{t0} (MPa)
Present study	660	54.8	73.6	11516	11709
ABNT NBR 7190 (ABNT, 1997)	694	59.8	75.5	12912	------
Christoforo, Almeida, Varanda, Panzera, and Lahr (2020a)	690	------	------	------	------
Christoforo, Couto, Almeida, Aquino, and Lahr (2020b)	------	59.2	------	------	------
Dias et al. (2019)	730	65.5	------	------	------
Instituto de Pesquisas Tecnológicas (1981)	710	52.3	------	------	------
Dias and Lahr (2004)	663	58.0	71.0	11990	11096

Table 6. Results of properties obtained by different authors - Angelim Ferro.

Authors	$\rho_{ap\ (12\%)}$ (kg m^{-3})	f_{c0} (MPa)	f_{t0} (MPa)	E_{c0} (MPa)	E_{t0} (MPa)
Present study	1160	79.2	110.6	20648	19586
ABNT NBR 7190 (ABNT, 1997)	1170	79.5	117.8	20827	------
Christoforo et al. (2020a)	1170	------	------	------	------
Christoforo et al. (2020b)	------	79.5	------	------	------
Dias et al. (2019)	1160	------	------	------	------
Instituto de Pesquisas Tecnológicas (1981)	1170	79.5	117.8	20827	------
Grobério and Lahr (2002)	1170	79.1	117.9	20946	19788
Dias and Lahr (2004)	1163	82.0	115.0	21263	19750

Table 7. ANOVA results for the comparison between E_{c0} and E_{t0} - Angelim Pedra.

Source	GL	SQ (Aj.)	QM (Aj.)	Value F	Value P
Solicitation	1	926,984	926,984	0.20	0.654
Error	98	450,413,981	4,596,061	------	------
Total	99	451,340,965	------	------	------

Table 8. ANOVA results for the comparison between E_{c0} and E_{t0} - Angelim Ferro.

Source	GL	SQ (Aj.)	QM (Aj.)	Value F	Value P
Solicitation	1	28,200,348	28,200,348	2.36	0.128
Error	98	1,172,199,977	11,961,224	------	------
Total	99	1,200,400,325	------	------	------

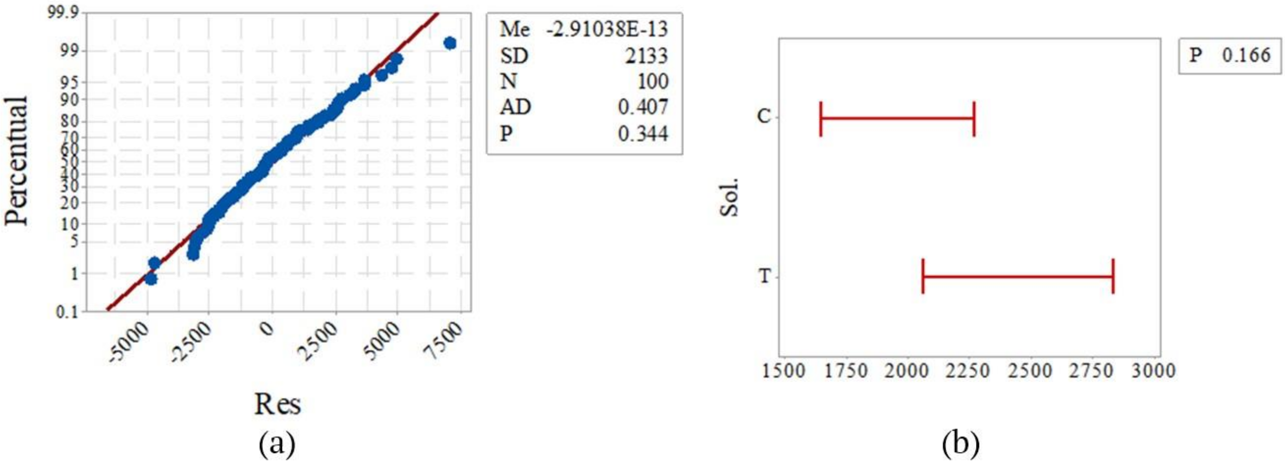

Figure 4. Results of normality tests (a) Homogeneity of variances (b) Residues related to the comparison of the E_{c0} and E_{t0} modulus of elasticity of Angelim Pedra.

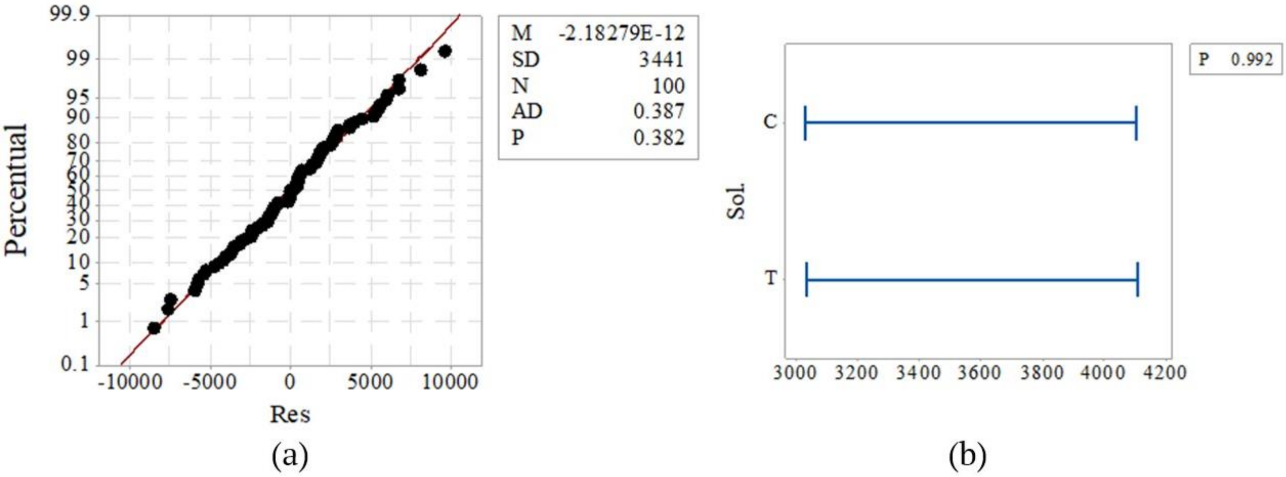

Figure 5. Results of normality tests (a) Homogeneity of variances (b) Residues related to the comparison of the E_{c0} and E_{t0} modulus of elasticity of Angelim Ferro.

In Figure 4 and 5, since P-values are higher than the level of significance adopted (5%), the normality and homogeneity of the variance of the residues validated the ANOVA results presented in Table 7 and 8. Based on Table 7 and 8, the equivalence of the E_{c0} and E_{t0} elasticity modulus for both wood species was found, a result following the established by the Brazilian standard ABNT NBR 7190 (ABNT, 1997). Tables 9, 10, 11, 12, 13 and 14 show the mean values (X_m), the standard deviations (SD), the lowest (Min), and the highest (Max) values, as well as the confidence interval of the mean (CI - 95% reliability) of the maximum displacements in the simulated structures (10 typologies) considering the mechanical properties of the two wood species (Angelim Pedra and Angelim Ferro) for the two spans evaluated (5 and 10 m).

It was observed in Table 9 to 14 that the displacement limit value (L/200) was exceeded in several models (57 out of 60 mean values - 95%). Another point to be emphasized is that 76% of the models in which modulus of elasticity was randomly assigned showed maximum displacement above the value defined by the Brazilian standard. The confidence intervals (CI) with 95% confidence were calculated, where 17.32, 30.18, and 34.80% were found above the reference limits for the spans of 5, 10, and 20 m, respectively. Such values were considerably higher than those calculated using the mean compression elasticity modulus parallel to the grain, as ABNT NBR 7190 (ABNT, 1997) recommended.

Table 9. Displacement results obtained: 5 m - Angelim Pedra.

Tip.	L/200	X_m (mm)	SD (mm)	Min (mm)	Max (mm)	CI (95%)
Porch	25.00	25.18	1.59	23.5	26.9	(23.59; 26.76)
Incl. Chord		26.52	1.33	24.3	27.9	(24.93; 28.10)
Par. Chord		26.04	1.23	24.0	27.3	(24.45; 27.62)
Top Chord		26.02	1.06	24.9	27.1	(24.42; 27.60)
Bowstring		26.46	2.23	24.3	29.8	(24.87; 28.04)
Fink		26.86	1.19	25.4	28.7	(25.27; 28.44)
Howe		27.74	3.08	23.4	30.5	(26.15; 29.33)
K Truss		25.32	0.76	24.2	26.2	(23.73; 26.90)
Pratt		26.00	2.33	23.3	29.1	(24.41; 27.59)
Scissor		27.36	1.45	25.9	28.9	(25.77; 28.94)

Table 10. Displacement results obtained: 5 m span - Angelim Ferro.

Tip.	L/200	X_m (mm)	SD (mm)	Min (mm)	Max (mm)	CI (95%)
Porch	25.00	24.48	1.36	22.6	26.0	(22.51; 26.44)
Incl. Chord		26.24	1.92	24.0	28.6	(24.27; 28.20)
Par. Chord		26.36	1.70	24.0	28.6	(24.39; 28.32)
Top Chord		26.30	1.82	23.9	28.6	(24.33; 28.26)
Bowstring		27.22	3.00	24.4	31.4	(25.26; 29.18)
Fink		25.42	1.29	24.2	27.4	(23.45; 27.38)
Howe		26.48	1.29	24.5	27.9	(25.35; 27.61)
K Truss		27.34	1.68	25.4	28.9	(25.37; 29.30)
Pratt		27.04	3.50	23.7	32.8	(22.51; 26.44)
Scissor		29.56	2.85	27.2	33.9	(24.27; 28.20)

Table 11. Displacement results obtained: 10 m span - Angelim Pedra.

Tip.	L/200	X_m (mm)	SD (mm)	Min (mm)	Max (mm)	CI (95%)
Porch	50.00	50.30	3.52	45.8	54.2	(46.54; 54.06)
Incl. Chord		53.04	3.67	48.8	56.7	(49.28; 56.80)
Par. Chord		54.66	6.94	46.1	63.7	(50.90; 58.42)
Top Chord		52.44	2.92	49.8	56.7	(48.68; 56.20)
Bowstring		55.62	3.43	53.0	60.5	(51.86; 59.38)
Fink		54.26	1.64	52.5	56.2	(50.50; 58.01)
Howe		54.68	2.51	52.1	58.8	(50.92; 58.44)
K Truss		51.08	1.55	49.4	52.7	(47.32; 54.83)
Pratt		54.98	7.25	47.7	65.6	(51.22; 58.74)
Scissor		55.24	3.78	50.9	60.2	(51.48; 59.00)

Table 12. Displacement results obtained: 10 m span - Angelim Ferro.

Tip.	L/200	X_m (mm)	SD (mm)	Min (mm)	Max (mm)	IC (95%)
Porch	50.00	54.24	7.03	48.5	66.5	(49.87; 58.61)
Incl. Chord		52.46	4.06	48.2	58.7	(48.90; 56.02)
Par. Chord		54.26	6.29	49.1	64.7	(49.89; 58.63)
Top Chord		54.94	2.66	51.2	57.6	(52.61; 57.27)
Bowstring		56.56	6.77	49.7	67.9	(52.19; 60.93)
Fink		54.16	3.25	51.3	59.4	(49.79; 58.53)
Howe		54.98	3.34	49.5	58.2	(50.61; 59.35)
K Truss		48.38	3.40	45.2	52.3	(44.01; 52.75)
Pratt		60.72	3.84	54.5	64.9	(56.35; 65.09)
Scissor		53.18	5.18	46.9	59.2	(48.81; 57.55)

In 56% of the cases, there were maximum displacements in the bottom chord and 44% in the top chord. Such excessive displacements in the bottom chord can generate pathologies in elements adjacent to the structure. Oliveira and Cardoso (2018) claim that excessive deflections can cause cracks and breaks in masonry due to incompatibility between the structures' deformations and the components that integrate the buildings. Cracks in the wood can cause the loss of strength of the element, affecting the performance of the entire structure. Also, excessive displacement in the top chord can cause the appearance of openings in the roof due to the lack of fit between the roof tiles, allowing infiltration into the building. The presence of moisture is one of the leading causes of pathologies in timber structures (Andrade Junior et al., 2012).

Table 13. Displacement results obtained: 20 m span - Angelim Pedra.

Tip.	L/200	X_m (mm)	SD (mm)	Min (mm)	Max (mm)	CI (95%)
Porch	100.00	105.74	13.12	88.20	120.10	(98.33; 113.15)
Incl. Chord		105.40	6.23	97.50	113.50	(97.99; 112.81)
Par. Chord		104.76	8.33	93.00	111.80	(97.35; 112.17)
Top Chord		99.38	7.99	89.10	110.20	(91.97; 106.79)
Bowstring		102.02	4.82	94.90	107.50	(94.61; 109.43)
Fink		109.54	6.53	98.30	115.10	(102.13; 116.95)
Howe		103.76	9.64	95.80	120.50	(96.35; 111.17)
K Truss		103.18	4.02	97.60	108.20	(95.77; 110.59)
Pratt		105.06	9.81	96.00	121.00	(97.65; 112.47)
Scissor		103.78	7.55	92.80	111.00	(96.37; 111.19)

Table 14. Displacement results obtained: 20 m span - Angelim Ferro.

Tip.	L/200	X_m (mm)	SD (mm)	Min (mm)	Max (mm)	CI (95%)
Porch	100.00	127.78	8.01	119.60	140.50	(120.76; 134.80)
Incl. Chord		107.76	8.79	98.10	120.50	(100.08; 115.44)
Par. Chord		104.22	6.36	95.30	112.80	(96.54; 111.90)
Top Chord		108.68	6.17	101.30	113.60	(101.00; 116.36)
Bowstring		102.62	10.84	88.00	115.60	(94.94; 110.30)
Fink		109.88	9.57	97.40	122.40	(102.20; 117.56)
Howe		106.54	7.68	98.50	115.20	(98.86; 114.22)
K Truss		106.76	4.08	100.90	110.70	(99.08; 114.44)
Pratt		105.12	9.51	98.70	121.80	(97.44; 112.80)
Scissor		103.90	10.51	98.30	122.50	(96.22; 111.58)

Based on the commented results, it was observed that the simplified method proposed by the Brazilian standard could generate excessive displacements in the timber structures. It contributes to the appearance of pathological manifestations in the structural elements and underlying elements such as frames, masonry, and other elements adjacent to the structure. Macchioni and Mannucci (2018) noted that excessive displacements could typically be related to individual elements' failure or risk of failure. Also, excessive displacement can cause structural problems (Calil Júnior et al., 2006).

Another point analyzed was comparing the stress of each compressed bar with the Euler load. In 59% of the cases analyzed, where the elasticity modulus for each truss bar was randomly adopted, at least one truss bar showed stress greater than the Euler load. It is worth mentioning that the loads proposed by ABNT NBR 7190 (ABNT, 1997) to verify the ultimate limit state of instability, considering possible second-order effects and element imperfections, are lower than those calculated by Euler's formula. Also, all modeled trusses were isostatic, implying that one element's failure would cause the entire structure to collapse.

Also, 81% of the models where the properties of the parts were randomly assigned showed displacement above L/200 or greater stress than Euler's critical load in at least one element. In other words, only 19% of the models did not present any type of problem. It is worth mentioning that it was considered that the connections remain integral, assuming that the failure occurs only in the timber bars (Christoforo, Romanholo, Panzera, Borges, & Lahr, 2011).

The results showed that the displacements were higher than the reference value in several models, and several bars showed greater stresses than the Euler load, indicating local instability of the structure. These results indicated that the adoption of $E_{c0,m}$ for all members could generate a higher stiffness of the structure than the actual value ('*in loco*') when the members are randomly positioned in the structure. These results also indicated that the method recommended by the standard could cause excessive displacements in timber trusses, which can influence performance and durability.

The literature review shows that several pathologies are caused by design failures, execution, lack of maintenance, and possible structural design mistakes. This research indicates that the methodology ABNT NBR 7190 (ABNT, 1997) recommended for calculating displacements in roof trusses can generate excessive displacements and local instabilities. An alternative is the pre-classification of structural elements, with the aid of non-destructive methods, which allows the choice of parts with higher quality for more critical positions, while parts of lower quality can be positioned in places of lower stresses. Several of the works mentioned above attested to the efficiency of such methods for estimating wood properties, so they are an efficient alternative to methods performed in the laboratory. Such measures can reduce the displacement of timber structures, reducing the appearance of pathologies.

The normative standard regulating the calculation of timber structures was published in 1997, which is more than two decades ago. In recent years the construction methods of different types of structures and materials have evolved and diversified. Structural systems and timber components will probably be increasingly used because they are environmentally, socially, and economically appropriate options (Bukauskas et al., 2019). Thus, it is essential to improve design methods to make such structures increasingly efficient. In the present study, it was observed that the adoption of $E_{c0,m}$ for all elements of the truss in the calculation of displacements could generate excessive displacements, causing pathologies. Pre-classification with non-destructive tests of the bar elements makes it possible to position rationally.

Conclusion

This study indicated that the methodology for calculating displacements recommended by ABNT NBR 7190 (ABNT, 1997) can cause excessive displacements. Confidence intervals showed values 17.32, 30.18, and 34.80% higher than the reference limits for spans of 5, 10, and 20 m, respectively.

Non-destructive techniques can be used to obtain the wood’s modulus of elasticity. Based on that, parts with higher stiffness values can be positioned in regions with greater demand, preventing excessive deflections and pathologies resulting from excessive displacement. The rational arrangement is a relatively low-cost and straightforward measure, easily applicable in companies that produce such structures.

Acknowledgments

The authors thank the National Council for Scientific and Technological Development (CNPq) and the Coordination for the Improvement of Higher Education Personnel (CAPES) for the support provided.

References

Almeida, T. H., Almeida, D. H., Christoforo, A. L., Chahud, E., Branco, L. A. M. N., & Lahr, F. A. R. (2016). Density as estimator of strength in compression parallel to the grain in wood. *International Journal of Materials Engineering, 3*(6), 67-71. DOI: https://doi.org/10.5923/j.ijme.20160603.01

Andrade Junior, J. R., Almeida, D. H., Almeida, T. H., Christoforo, A. L., Stamato, G. C., & Lahr, F. A. R. (2014). Avaliação das estruturas de cobertura em madeira de um galpão de estoque de produtos químicos. *Ambiente Construído, 14*(3), 75-85. DOI: https://doi.org/10.1590/S1678-86212014000300006

Andrade Junior, J. R., Almeida, D. H., Stamato, G. C., Christoforo, A. L., & Lahr, F. A. R. (2012). Avaliação das condições estruturais de telhados construídos com madeira brasileira nativa. *Madeira: Arquitetura e Engenharia, 13*(32), 1-10.

Associação Brasileira de Normas Técnicas [ABNT]. (1997). *NBR 7190: projeto de estruturas de madeira*. Rio de Janeiro, RJ: ABNT.

Ballarin, A. W., & Palma, H. A. L. (2009). Avaliação do módulo de elasticidade de madeiras de reflorestamento com uso do método não destrutivo de vibração transversal. *Madeira: Arquitetura e Engenharia, 10*(25), 5-14.

Ballarin, A. W., Palma, H. A. L., & Hellmeister, L. A. V. (2010). Ensaios não-destrutivos de propagação de ondas em toras e madeira serrada de Pinus. taeda L. *Madeira: Arquitetura e Engenharia, 11*(26), 17-30.

Branco, J. M., Sousa, H. S., & Tsakanika, E. (2017). Non-destructive assessment, full-scale load-carrying tests and local interventions on two historic timber collar roof trusses. *Engineering Structures, 140*, 209-224. DOI: https://doi.org/10.1016/j.engstruct.2017.02.053

Bukauskas, A., Mayencourt, P., Shepherd, P., Sharma, B., Mueller, C., Walker, P., & Bregulla, J. (2019). Whole timber construction: a state of the art review. *Construction and Building Materials, 213*, 748-769. DOI: https://doi.org/10.1016/j.conbuildmat.2019.03.043

Calil Júnior, C., Dias, A. A., Góes, J. L. N., Cheung, A. B., Stamato, G. C., Pigozzo, J. C., ... Lana, É. L. (2006). *Manual de projeto e construção de pontes de madeira*. São Carlos, SP: Suprema.

Castellanos, J. R. S. (2020). Módulo dinámico de la madera laminada compuesta de tres especies, determinado por vibraciones transversales. *Pistas Educativas, 135*, 276-288.

Cavalheiro, R. S., Almeida, D. H., Almeida, T. H., Araújo, V., Christoforo, A. L., & Lahr, F. A. R. (2016). Mechanical properties of Paricá wood using structural members and clear specimens. *International Journal of Materials Engineering, 6*(2), 56-59. DOI: https://doi.org/10.5923/j.ijme.20160602.06

Chen, Y., & Guo, W. (2016). Mechanical properties evaluation of two wood species of ancient timber structure with nondestructive testing methods. *BioResources, 11*(3), 6600-6612. DOI: https://doi.org/10.15376/biores.11.3.6600-6612

Christoforo, A. L., Almeida, D. H., Varanda, L. D., Panzera, T. H., & Lahr, F. A. R. (2020a). Estimation of wood toughness in Brazilian tropical tree species. *Engenharia Agrícola, 40*(2), 232-237. DOI: https://doi.org/10.1590/1809-4430-Eng.Agric.v40n2p232-237/2020

Christoforo, A. L., Couto, N. G., Almeida, J. P. B., Aquino, V. B. M., & Lahr, F. A. R. (2020b). Apparent density as an estimator of wood properties obtained in tests where failure is fragile. *Engenharia Agrícola, 40*(1), 105-112. DOI: https://doi.org/10.1590/1809-4430-Eng.Agric.v40n1p105-112/2020

Christoforo, A. L., Romanholo, G. A., Panzera, T. H., Borges, P. H. R., & Lahr, F. A. R. (2011). Influence of stiffness in bolted connections in wooden plane structure of truss type. *Engenharia Agrícola, 31*(5), 998-1006. DOI: https://doi.org/10.1590/S0100-69162011000500017

Dias, F. M., Almeida, T. H., Araújo, V. A., Panzera, T. H., Christoforo, A. L., & Lahr, F. A. R. (2019). Influence of the apparent density on the shrinkage of 43 tropical wood species. *Acta Scientiarum. Technology, 41*(1), e30947. DOI: https://doi.org/10.4025/actascitechnol.v41i2.30947

Dias, F. M., & Lahr, F. A. R. (2004). Estimativa de propriedades de resistência e rigidez da madeira através da densidade aparente. *Scientia Forestalis*, *65*, 102–113.

Dietsch, P. (2011). Robustness of large-span timber roof structures - structural aspects. *Engineering Structures, 33*(11), 3106-3112. DOI: https://doi.org/10.1016/j.engstruct.2011.01.020

Faydi, Y., Brancheriau, L., Pot, G., & Collet, R. (2017). Prediction of oak wood mechanical properties based on the statistical exploitation of vibrational response. *BioResources, 12*(3), 5913-5927. DOI: https://doi.org/10.15376/biores.12.3.5913-5927

Garcia, R. A., Carvalho, A. M., Latorraca, J. V. F., Matos, J. L. M., Santos, W. A., & Silva, R. F. M. (2012). Nondestructive evaluation of heat-treated *Eucalyptus grandis* Hill ex Maiden wood using stress wave method. *Wood Science and Technology, 46*(1-3), 41-52. DOI: https://doi.org/10.1007/s00226-010-0387-6

Guan, C., Liu, J., Zhang, H., Wang, X., & Zhou, L. (2019). Evaluation of modulus of elasticity and modulus of rupture of full-size wood composite panels supported on two nodal-lines using a vibration technique. *Construction and Building Materials, 218*, 64-72. DOI: https://doi.org/10.1016/j.conbuildmat.2019.05.086

Grobério, M. P., & Lahr, F. A. R. (2002). Indicações para o emprego da madeira de espécies tropicais do Brasil. *Madeira: Arquitetura e Engenharia*, *3*(8).

Haines, D. W., Leban, J.-M., & Herbé, C. (1996). Determination of Young's modulus for spruce, fir and isotropic materials by the resonance flexure method with comparisons to static flexure and other dynamic methods. *Wood Science and Technology, 30*, 253-263. DOI: https://doi.org/10.1007/BF00229348

Instituto de Pesquisas Tecnológicas [IPT]. (1981). *Informações sobre madeiras*. São Paulo, SP: IPT.

Macchioni, N., & Mannucci, M. (2018). The assessment of Italian trusses: survey methodology and typical pathologies. *International Journal of Architectural Heritage, 12*(4), 533-544. DOI: https://doi.org/10.1080/15583058.2018.1442516

Martins, C., Dias, A. M. P. G., & Cruz, H. (2019). Using non-destructive testing to predict the mechanical properties of glued laminated poplar. *Proceedings of the Institution of Civil Engineers: Structures and Buildings, 172*(9), 661-670. DOI: https://doi.org/10.1680/jstbu.18.00060

Matos, G. S. B., Silva, G. R., Gama, M. A. P., Vale, R. S., & Rocha, J. E. C. (2012). Desenvolvimento inicial e estado nutricional de clones de eucalipto no nordeste do Pará. *Acta Amazônica, 42*(4), 491-500. DOI: https://doi.org/10.1590/S0044-59672012000400006

Mori, M., Hasegawa, M., Yoo, J.-C., Kang, S.-G., & Matsumura, J. (2016). Nondestructive evaluation of bending strength of wood with artificial holes by employing air-coupled ultrasonics. *Construction and Building Materials, 110*, 24-31. DOI: https://doi.org/10.1016/j.conbuildmat.2016.02.020

Oliveira, T. S., & Cardoso, A. C. S. (2018). Deformação lenta das estruturas de concreto armado e suas manifestações patológicas. *Revista de Engenharia e Tecnologia, 10*(3), 195-206.

Pinheiro, R. V., Lázaro, L. G. F., Macedo, L. B., Christoforo, A. L., & Lahr, F. A. R. (2016). Repair methods indication for a timber coverage structure located in sinop city - Brazil. *International Journal of Materials Engineering, 6*(2), 39-46. DOI: https://doi.org/10.5923/j.ijme.20160602.03

Sandak, A., Sandak, J., & Riggio, M. (2015). Assessment of wood structural members degradation by means of infrared spectroscopy: an overview. *Structural Control and Health Monitoring*, *23*, 396-408. DOI: https://doi.org/10.1002/stc.1777

Segundinho, P. G. A., Carreira, M. R., Calil Neto, C., Regazzi, A. J., Dias, A. A., & Calil Junior, C. (2013). Avaliação do módulo de elasticidade de peças de madeira laminada colada (MLC) obtido por meio do ensaio de vibração transversal. *Ambiente Construído, 13*(2), 7-14. DOI: https://doi.org/10.1590/S1678-86212013000200002

Ter Steege, H., Vaessen, R. W., Cárdenas-Lópes, D., Sabatier, D., Antonelli, A., Oliveira, S. M., ... Salomão, R. P. (2016). The discovery of the Amazonian tree flora with an updated checklist of all known tree taxa. *Scientific Reports, 6*, 29549. DOI: https://doi.org/10.1038/srep29549

Trevisan, H., Tieppo, F. M. M., Carvalho, A. G., & Lelis, R. C. C. (2007). Avaliação de propriedades físicas e mecânicas da madeira de cinco espécies florestais em função da deterioração em dois ambientes. *Árvore, 31*(1), 93-101. DOI: https://doi.org/10.1590/S0100-67622007000100011

Tuisima-Coral, L. L., Odicio-Guevara, J. E., Weber, J. C., Lluncor-Mendonza, D., & Lojka, B. (2017). Variación de las propiedades físicas en troncos de Guazuma crinita, una especie maderable en el Amazonas Peruano. *Madera y Bosques, 23*(1), 53-61. DOI: https://doi.org/10.21829/myb.2017.2311534

Yang, Z., Jiang, Z., Hse, C. Y., & Liu, R. (2017). Assessing the impact of wood decay fungi on the modulus of elasticity of slash pine (*Pinus elliottii*) by stress wave non-destructive testing. *International Biodeterioration & Biodegradation, 117*, 123-127. DOI: https://doi.org/10.1016/j.ibiod.2016.12.003

Zangiácomo, A. L., Christoforo, A. L., & Lahr, F. A. R. (2016). Elasticity moduli in round wooden beams of Pinus caribaea. *Engenharia Agrícola, 36*(3), 566-570. DOI: https://doi.org/10.1590/1809-4430-Eng.Agric.v36n3p566-570/2016